The surface science of quasicrystals

2010 J. Phys.: Condens. Matter 22 084022

(http://iopscience.iop.org/0953-8984/22/8/084022)

J. Phys.: Condens. Matter **22** (2010) 084022 (14pp) doi:10.1088/0953-8984/22/8/084022

The surface science of quasicrystals

R McGrath[1,4], J A Smerdon[1], H R Sharma[1], W Theis[2] and J Ledieu[3]

[1] Department of Physics and Surface Science Research Centre, The University of Liverpool, Liverpool L69 3BX, UK
[2] The Nanoscale Physics Research Laboratory, The School of Physics and Astronomy, The University of Birmingham, Edgbaston, Birmingham B15 2TT, UK
[3] Institut Jean Lamour, UMR7198 CNRS-Nancy Université-UPVM, Ecole des Mines, Parc de Saurupt, F-54042 Nancy, France

E-mail: mcgrath@liv.ac.uk

Received 3 February 2009, in final form 26 May 2009
Published 5 February 2010
Online at stacks.iop.org/JPhysCM/22/084022

Abstract
The surfaces of quasicrystals have been extensively studied since about 1990. In this paper we review work on the structure and morphology of clean surfaces, and their electronic and phonon structure. We also describe progress in adsorption and epitaxy studies. The paper is illustrated throughout with examples from the literature. We offer some reflections on the wider impact of this body of work and anticipate areas for future development.

(Some figures in this article are in colour only in the electronic version)

1. Introduction

Quasicrystals are intermetallic alloys which have excellent long-range order but without translational symmetry. Consequently they can have rotational symmetries once thought to be disallowed under the rules of crystallography. They were discovered in 1982 [1], and this led to a surge in activity as workers attempted to solve their complex structures and to measure and understand their unusual physical properties. The scanning tunnelling microscope (STM) was also invented in the early 1980s and the first publication using this technique was in 1982 [2]. This coincidence of discovery has had significant impact for the study of quasicrystal surfaces. The first structural study of a quasicrystal surface was carried out in 1990 by a group at AT&T Bell laboratories. That work, entitled 'Real space atomic structure of a two-dimensional quasicrystal: $Al_{65}Cu_{20}Co_{15}$' used STM to image the surface [3]. A step-terrace morphology was observed, and images with good resolution of individual terraces revealed atomic detail which was compared to structural models. Not only was this the first STM data from a quasicrystal surface, this paper also introduced the use of image analysis techniques such as Fourier filtering which were employed in many later studies. A description of image analysis techniques applied to quasicrystals has been given elsewhere [4]. A low energy electron diffraction (LEED) study on this surface was also published by the same group [5].

The first STM study of the surface of an icosahedral quasicrystal was published in 1994 by Schaub and co-workers, using STM [6]. Although the resolution was not optimum by today's standards, several structural motifs were identified. In particular Schaub *et al* showed that the pentagonal hollows (later dubbed 'dark stars' [7]) form a Fibonacci pentagrid, compelling evidence that the surface itself is quasicrystalline.

Building on these early successes, there is now a substantial body of literature on these surfaces. In this paper we review the most studied clean surfaces and then summarize work on adsorption and epitaxy. This is not intended to be a comprehensive review, rather a snapshot of the state-of-the-art in the field. The final section addresses some broader issues, such as connections with the wider field of surface science and areas with the best potential for future progress.

2. Clean surfaces—structure and morphology

2.1. The fivefold surface of icosahedral Al–Pd–Mn

Up to now, the fivefold surface of the icosahedral Al–Pd–Mn sample remains the most studied quasicrystalline surface. It is reasonable to say that the atomic surface structure is relatively well understood. With micrometre-sized atomically flat terraces prepared routinely, this surface is nowadays

[4] Author to whom any correspondence should be addressed.

intensively used as a quasiperiodic template for adsorption studies and film growth [8, 9].

One of the major hurdles in studying quasicrystalline surfaces has been the surface preparation. Enrichment or depletion of one element at the surface shifts the overall composition away from the narrow icosahedral region of the phase diagram and several phases have been observed on the fivefold $Al_{70}Pd_{21}Mn_9$ surface. Upon sputtering, preferential removal of the lightest element leads to the formation of grains of crystalline β-AlPd phase of CsCl-type structure with either the [110] or the [113] directions normal to the surface [10–13]. Here, the apparent tenfold pattern recorded using low energy electron diffraction (LEED) derives from five cubic domains rotated from each other by 72°. Similarly, a decagonal epilayer of composition equal to $Al_{22}Pd_{56}Mn_{22}$ can be formed while ion bombarding the sample held between 500 and 700 K [14]. In all cases, annealing the sample above 700 K for several hours restores the nominal bulk composition and a quasiperiodic order at the surface. However, two different topographies have been observed by scanning tunnelling microscopy (STM) depending on the annealing parameters [15]. For annealing temperatures ranging between 700 and 830 K, the surface is rough and reveals cluster like protrusions. The LEED pattern is sharp and quasiperiodic in nature. The topography is comparable to the surface obtained by cleaving and subsequent annealing to 800 K [16].

To produce large atomically flat terraces [17] on the $Al_{70}Pd_{21}Mn_9$ quasicrystal surface, cycles of sputtering and annealing between 830 and 930 K for several hours are required (annealing to higher temperatures leads to evaporation of selected elements and to the formation of crystalline phases [18]). Following this surface preparation and using dynamical LEED analysis, Gierer *et al* [19] concluded that the surface of the $Al_{70}Pd_{21}Mn_9$ is bulk-terminated, i.e the surface planes are identical to planes from the bulk model. The two topmost layers are contracted by 0.1 Å compared to the bulk spacing and their combined density is equal to 0.135 atom $Å^{-2}$. The topmost plane is Al rich and the layer 0.38 Å beneath has the composition $Al_{50}Pd_{50}$. The interlayer relaxation and the proposed layer composition are also supported by ion scattering experiments [20, 21]. Atomically resolved STM images have been obtained and compared to existing theoretical models [17, 22]. All STM analyses reported so far suggest that the topmost surface is indeed bulk-terminated [17, 22].

Along the fivefold direction of the i-Al–Pd–Mn bulk model, the structure can be visualized as blocks of atomic layers separated by interlayer spacings (gaps) of various width and appearing in a Fibonacci sequence. From a step height distribution study on the i-Al–Cu–Fe surface (isostructural to the i-Al–Pd–Mn quasicrystal) [23], it is suggested that the surface planes correspond to bulk truncations at large gaps above regions of relatively large atomic density or of high Al content. The terraces are separated mainly by two step heights namely $L = 6.6$ Å and $M = 4.1$ Å which form a Fibonacci sequence ($\cdots LMLLMLMLLM \cdots$) [6, 24]. An additional step height S equal to 2.4 Å ($\approx L$–M) is also observed but less frequently [25]. The step height ratio L/M approaches the golden mean τ ($=1.618\cdots$), an irrational number intrinsic to the quasicrystalline structure. Compared to crystalline materials, the step morphologies of the $Al_{70}Pd_{21}Mn_9$ surface are considerably different. The steps often meander, intersect and the large-scale roughness associated with both L and M steps is believed to be intrinsic to the quasicrystalline surface. This roughness reflects a non-equilibrium structure frozen-in during the cooling from an equilibrium structure at the annealing temperature used for the surface preparation towards a different equilibrium structure at lower temperature which is not reached due to insufficient diffusivity at the lower temperatures. The step diffusivity on this surface increases as the step height decreases. Step edges exhibit local facetting on the order of a few tens of angstroms with the linear segments orientated in the direction of highest atomic density [24].

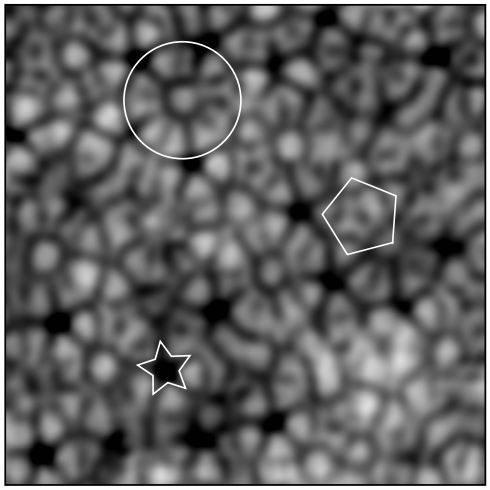

Figure 1. 8 nm × 8 nm high resolution STM image obtained on the fivefold $Al_{70}Pd_{21}Mn_9$ surface. A regular pentagon used in the Penrose P1 tiling, a 'dark star' (DS) and a 'white flower' (WF) are outlined.

We now focus on the atomic decoration of individual terraces. To this end, STM has been one of the most valuable tools to characterize the local structural arrangement of this aperiodic surface [17, 22]. To interpret the atomic structure observed on the $Al_{70}Pd_{21}Mn_9$ surface, a tiling approach was first employed. Connecting points of high contrast on STM images to create pentagons led to the formation of a Penrose (-P1) like tiling consisting of rhombuses, pentagonal stars, regular pentagons (highlighted on figure 1) and crowns [17, 26]. The good agreement between the experimental P1 tiling and the theoretical tiling derived from the geometric model of the bulk provided further support (this time in real space) for a bulk truncated surface. Within terraces, several characteristic motifs have been identified and have been called 'dark stars' (DS), 'white flowers' (WF) and 'rings' (R) [6, 17]. The presence of the R pattern (not shown here) is terrace-dependent and varies with the annealing conditions [27].

The origin of the DS and WF motifs remains subject to debate [28]. The real-space bulk structure is built on the interpenetration of two types of clusters, the Bergman (33 atoms) and pseudo-Mackay (50 atoms) clusters. Theses

highly symmetric elementary units are regarded as basics building blocks for this aperiodic alloy. The Bergman cluster consists of a central atom surrounded by an icosahedron (12 atoms) and by a dodecahedron (30 atoms) as an outer shell. The pseudo-Mackay cluster is described by an central atom surrounded by a partially occupied dodecahedron (7 atoms), by an icosahedron (12 atoms) as intermediate shell and by an icosidodecahedron (30 atoms) as an outer shell [29]. To generate atomic flat surfaces, these concentric units have to be dissected at different heights. Hence, the patterns observed by STM are related to the atomic decoration within these concentric units. Depending on the bulk structure models considered, several atomic arrangement have been proposed for instance to interpret the origin of the DS motifs [30, 31]. As it will be shown later, the DS and WF features play a major role in adsorption studies. They have also been discussed recently by Unal *et al* [28, 32].

From a theoretical viewpoint, *ab initio* density functional theory (DFT) calculations are nowadays feasible and have been carried out on so-called approximants [31]. An approximant can be described as a periodic crystal having a large unit cell within which the substructure is based on similar cluster types as those found in an aperiodic sample. The overall chemical composition of this periodic model is also very close to the parent quasicrystal. Upon surface relaxation, the *ab initio* calculations show that the skeleton of the P1 tiling decorated by transition-metal atoms at its vertices is preserved while considerable rearrangement of Al atoms are observed within the tiles along with large relaxations of the interlayer spacing [31]. The electronic charge density distribution calculated for the structure exhibits minima at the P1 vertices (position of Pd atoms 0.38 Å below the topmost surface layer) and strong charge depletions inside some of the pentagonal tiles. These charge density minima originate from structural vacancies due to the incomplete decoration of the first atomic shell of the pseudo-Mackay cluster. Following these calculations, simulated STM images have been generated. The DS and WF are well reproduced in the theoretical images and are related respectively to surface vacancies and to equatorially truncated pseudo-Mackay clusters surrounded by cut Bergman clusters [33]. The good agreement between experimental and simulated STM images reinforces the validity of using approximants as a first model in theoretical studies of quasicrystalline surfaces.

2.2. Decagonal Al–Ni–Co

Decagonal quasicrystals consist of quasicrystalline planes stacked periodically along a tenfold axis (along the decagonal rod in figure 2). Perpendicular to the unique tenfold axis, there exist two inequivalent sets of twofold axes. One set is perpendicular to the faces of the decagonal rod. The other set is rotated by 18° with respect to the former set. These axes can be labelled by generalized Miller indices [00001], [10000] and [00$1\bar{1}$0] respectively.

Al–Ni–Co exhibits a number of different decagonal phases depending on the exact composition and temperature ([9] and references therein). Surface studies have been performed

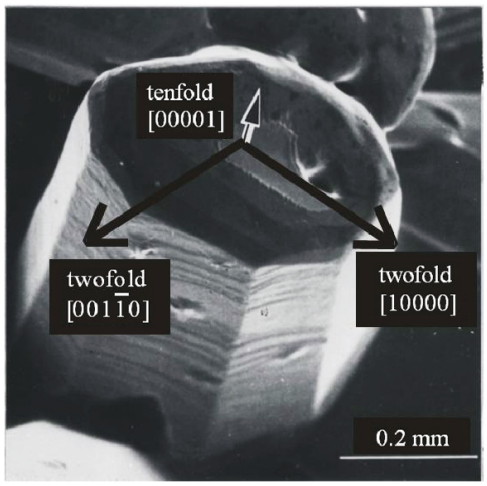

Figure 2. Scanning electron microscopy (SEM) micrograph showing an as-grown single grain sample of d-Al–Ni–Co quasicrystal [34]. High symmetry axes are labelled.

on two of these phases, the type-I superstructure phase [35] and the Co-rich phase [36–40]. These phases share common structural features.

The interplanar distance along the periodic axis is approximately 2 Å [41]. The structure can be described by columnar clusters of 20 Å diameter [42, 43]. The cluster in each plane has pentagonal symmetry. However, it is rotated by 36° with respect to the cluster in the neighbouring plane, yielding an overall tenfold symmetry in the diffraction pattern. The cluster centres form the vertices of a tiling. The tiling is different for different phases. The type-I superstructure phase is characterized by a rhombic Penrose tiling (consisting of two types of rhombi packed with a specific rule) [43], while the Co-rich phase is characterized by a pentagonal tiling (formed by a fat rhombus, a skinny rhombus and a pentagon tile) [44]. The distribution of atoms in the clusters differs from one phase to another.

2.2.1. The tenfold surface. The tenfold surface has been investigated intensively using a wide variety of techniques. The surface can be prepared with high structural quality. Helium atom scattering (HAS) shows a specular (reflected peak) intensity comparable to that of high-quality cleaved surfaces of periodic crystals, e.g., GaAs(110) [45]. LEED patterns from the surface show a dense pattern of spots distributed with symmetry expected from the bulk [35]. An example of a spot-profile-analysis-LEED image from the tenfold surface of the type-I superstructure is given in figure 3. All diffraction spots can be indexed using the surface projected basis vectors of the bulk, suggesting that the surface corresponds to a bulk truncation without surface reconstruction. The tenfold surface of the Co-rich phases studied by LEED, STM, low energy ion scattering (LEIS) [37, 39, 40] and ion scattering spectroscopy (ISS) [46] also show characteristics of the bulk truncation.

STM shows wide terraces separated by steps of 2 Å height [35, 37, 39, 40]. High resolution images show pentagonal features, which have the same orientation in a

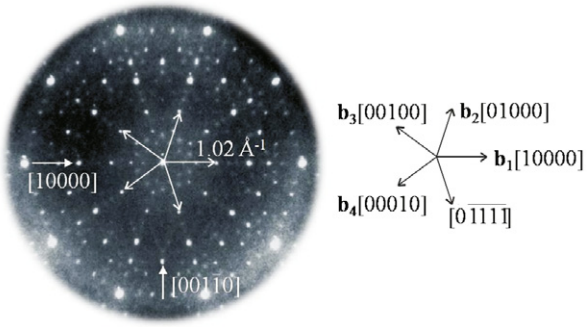

Figure 3. SPA-LEED image of the tenfold (00001) surface of d-$Al_{71.8}Ni_{14.8}Co_{13.4}$. The vectors $b_j = b(\cos\frac{2\pi j}{5}, \sin\frac{2\pi j}{5}, 0)$ with $j = 1, \ldots, 4$ and $b = 1.02$ Å^{-1} are the surface projected bulk basis vectors. Reprinted with permission from [47]. Copyright 2004, American Physical Society.

single terrace, but are rotated by 36° (inversion symmetry) in neighbouring terraces. The fine structure of the type-I superstructure phase can be overlaid by a randomized Penrose tiling of 20 Å edge length (figure 4). In contrast, high resolution STM images of the Co-rich phase can be characterized by a random pentagonal tiling [39]. Kortan *et al* also identified by STM a pentagonal tiling in the d-Al–Cu–Co quasicrystal [3, 48]. All observed features; the step height, the inversion symmetry and the tilings can be explained by a bulk truncated surface of the respective phase.

An *ab initio* study of the surface based on a model structure derived from the structure of the W–Al–Ni–Co approximant phase, has shown that the tunnelling current is predominantly contributed by the s–p electrons in Al atoms and thus brighter contrasts observed in STM images are mostly related to the Al atom sites [49]. The comparison of high resolution STM images with the atomic structure of the bulk truncated surface also reveals that most of the brighter parts are related to Al sites [39, 47].

Surface reconstruction and relaxation are common surface structural phenomena observed in periodic crystals. As described above, no surface reconstruction has been identified on the tenfold surfaces of decagonal quasicrystals. However, the surface is found to exhibit surface relaxation. Ferralis *et al* have shown on the basis of dynamical LEED analysis that the basic Co-rich phase displays a 10% contraction of the outermost layer spacing with respect to the bulk interlayer spacing [40]. The next layer spacing is expanded by 5%, whereas the remaining interlayer spacings are close to the bulk value.

2.2.2. The twofold surfaces. Both twofold (10000) and (00$1\bar{1}$0) surfaces have been investigated by HAS, SPA-LEED and STM [37, 47, 50–53]. These surfaces contain both periodic and quasiperiodic directions, thus providing an opportunity to study the influence of both crystalline and quasicrystalline order on physical properties. (See the discussion on frictional properties in section 6.) HAS and STM reveal that the (00$1\bar{1}$0) surface develops facets of the (10000) orientation [50, 53]. The facet planes are identical to those developed during crystal growth (figure 2), suggesting that the facets are formed due to the lower surface energy of the (10000) surface compared with that of the (10$1\bar{1}$0) surface. The observed structure features of both surfaces can be explained by bulk truncations.

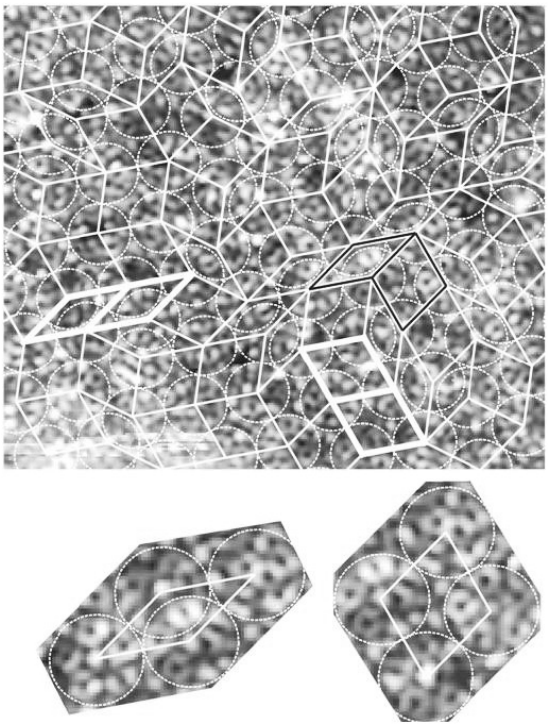

Figure 4. High resolution STM image of the tenfold d-$Al_{71.8}Ni_{14.8}Co_{13.4}$ (00001) surface (16 nm × 13 nm). Clusters marked by circles are located at the vertices of a rhombic Penrose tiling. A magnified skinny and a fat rhombus are shown in the bottom. The tiles with thick white edges show a configuration, which breaks a matching rule of the Penrose tiling. Reprinted with permission from [35]. Copyright 2004, American Physical Society.

2.3. Other quasicrystals

Sharma *et al* reported the first ultra-high vacuum (UHV) surface studies of a non-Al-based quasicrystal, namely i-$Ag_{42}In_{42}Yb_{16}$ [54]. This system is isostructural to the binary i-Cd-Yb quasicrystal and thus differs in terms of structure and chemistry from all previously investigated quasicrystals under UHV.

The surface can be prepared using the usual sputter-annealing technique. The sputtering preferentially removes In and Yb and quasicrystalline order is lost in the surface region. However, annealing recovers the bulk concentration and quasicrystalline order in the surface. A LEED pattern taken from the surface after annealing at 400 °C is given in figure 5 which shows the fivefold symmetry expected from the bulk structure.

STM images from the surface show up to several hundred nm large terraces separated by steps of three different heights: $S = 0.28$ nm, $M = 0.58$ nm, $L = 0.85$ nm. The S-steps are most frequently observed, whereas the M-steps are very rare. The size of terraces is comparable to those of Al-based quasicrystals. The step heights and their occurrence

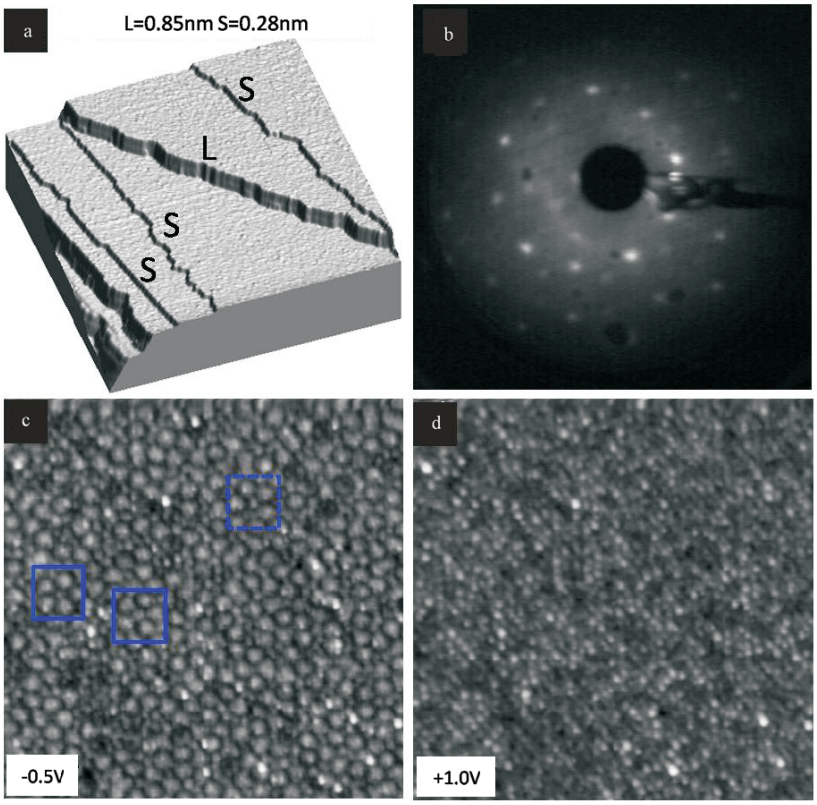

Figure 5. (a) STM image of the fivefold i-$Ag_{42}In_{42}Yb_{16}$ surface (250 nm × 250 nm). (b) LEED pattern from the same surface (electron energy 23 eV). (c), (d) Fine structure on a terrace at a negative bias voltage (c) and at a positive bias voltage (d) to the sample (49 nm × 49 nm).

are consistent with the separation of bulk planes which are relatively dense and rich in the low surface energy elements In and Yb. The high resolution STM images can be explained by the atomic structure of these planes. It has been shown that the tunnelling current from Yb sites is enhanced at positive bias voltage applied to the sample and suppressed at negative bias, while the tunnelling current from Ag or In sites behaves oppositely [55].

Finally, as reported in [56], both step height distribution and high resolution images of the fivefold surfaces of icosahedral Al–Cu–Fe and Al–Cu–Ru quasicrystals were found to be similar to those in i-Al–Pd–Mn.

3. Clean surfaces—electronic structure

The physical properties of a single crystal are determined to a large degree by its electronic structure. For quasicrystals, in particular the central question of the origin of their thermodynamic stability is intricately linked to their bulk electronic structure. The established method to study the latter experimentally is by angle resolved photoelectron spectroscopy (ARPES) from clean surfaces of single grain samples. In periodic crystals ARPES provides the electronic bulk band structure as well as the dispersion of any surface states or surface resonances. The photoelectrons detected in these experiments typically have inelastic mean free paths in the samples smaller than 10 Å. Thus, the bulk electronic structure is sampled in the top few atomic layers from the surface. While this has no impact on the interpretation of data from periodic metallic crystals, it does provide a potential challenge for quasicrystals.

This became apparent from early ARPES experiments [57–60] exploring the existence of a pseudogap in the density of states (DOS) at the Fermi energy E_F in icosahedral quasicrystals. While there was evidence for a pseudogap in all of these studies, there seemed to be some discrepancy regarding its magnitude. This was resolved by a core level photoemission study which found an enhanced core hole screening in the near surface region reflecting an increased DOS(E_F) close to the surface [61]. Thus the pseudogap signature in the valence band spectra becomes more pronounced for very low photon energies (13 eV in [57]) as the resulting photoelectrons have longer inelastic free paths and sample regions further from the surface. The position and width of the pseudogap of i-$Al_{70.5}Pd_{21}Mn_{8.5}$ were determined by experiments performed at elevated sample temperatures (570 K) to provide sufficient thermal occupation of states above E_F for photoemission [61]. Using a photon energy of 32.3 eV a shallow dip in the DOS was found centred slightly above E_F by 90 meV. Valence band photoemission data recorded at low temperature and modelled by a Lorentzian shaped pseudogap centred at E_F indicate pseudogap widths on the order of 0.2–0.4 eV for a wide range of different icosahedral quasicrystals [60].

A detailed understanding of the pseudogap and its decrease when sampled with higher surface sensitivity would

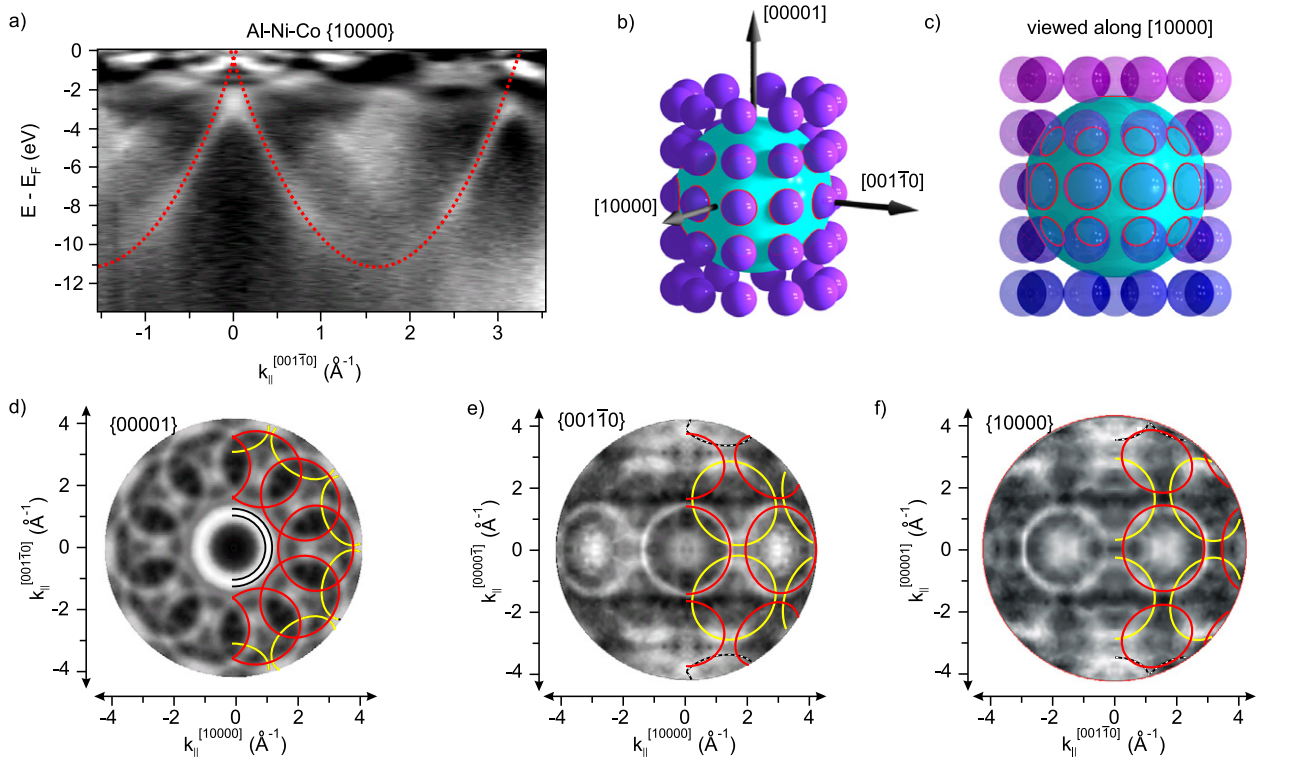

Figure 6. Valence band photoemission of d-Al–Ni–Co. (a) Band map along the quasiperiodic [001$\bar{1}$0] direction depicting parabolic nearly-free-electron bands. (b) and (c) *k*-space model depicting initial states of fixed binding energy (small spheres), final states of fixed kinetic energy (large sphere) and allowed transitions where these coincide (red circles). (d)–(f) Experimental photoemission intensity maps for the different high symmetry surfaces (background subtracted and normalized). Adapted from [64].

require a characterization of the spatial extent of the individual electronic states and their corresponding DOS. This has not been achieved for the icosahedral quasicrystals to date.

While electronic states in periodic crystals can be described by Bloch states identified by crystal momentum and band index yielding only delocalized bulk states and surface and surface resonance states, the situation is less straightforward for quasicrystals. If we were to consider only very weak pseudopotentials we would encounter delocalized bulk states (without well-defined crystal momentum) and possibly surface states and surface resonances. In this case, the decrease of the pseudogap under more surface sensitive conditions would be explained by enhanced contributions from surface states and resonances [61]. If, on the other hand, the bulk electronic states are critical, i.e. falling off with a power law [62], then the average local DOS and pseudogap signature would be expected to gradually change as the distance to the surface increases and the local critical states become less influenced by the cutoff at the receding surface.

The most common explanation for the origin of the pseudogap is interference of states at pseudo-Brillouin zone boundaries localized halfway between reciprocal lattice vectors with high structure factor [63]. This requires a band like dispersion of the states which both delocalized and critical states could provide. In icosahedral quasicrystals a single dispersing feature was reported in valence band photoemission at 2 eV binding energy [59], but not much progress has been made beyond this.

For decagonal quasicrystals, however, photoemission experiments have been able to provide a detailed understanding of their electronic structure. The most comprehensively studied decagonal quasicrystal is d-$Al_{71.8}Ni_{14.8}Co_{13.4}$. Photoemission experiments from the three low index surfaces revealed a nearly-free-electron like dispersion in the region of s–p derived states with the bands centred at reciprocal lattice points with large structure factor [64, 65] (see figure 6). The strong dispersion illustrates the non-localized character of the contributing electronic states. The experimental dispersion can be understood in a pseudopotential picture with the electronic states described by sums of only a few significant Fourier components each [66, 67]. The lack of observable gaps at crossing points of the bands indicates fairly weak pseudopotentials. The experiments cannot distinguish between different types of non-localized states, thus the states could be either delocalized or critical in character.

While in icosahedral quasicrystals the partial masking of the pseudogap revealed a clear change in the local DOS near the surface, there is no such evidence for the decagonal systems which do not feature pseudogaps. Their nearly-free-electron like band structure, however, might support surface states or surface resonances. Neither have been observed experimentally so far.

4. Clean surfaces—phonons

With the successful preparation of surfaces with high structural quality, it became possible to measure low energy surface

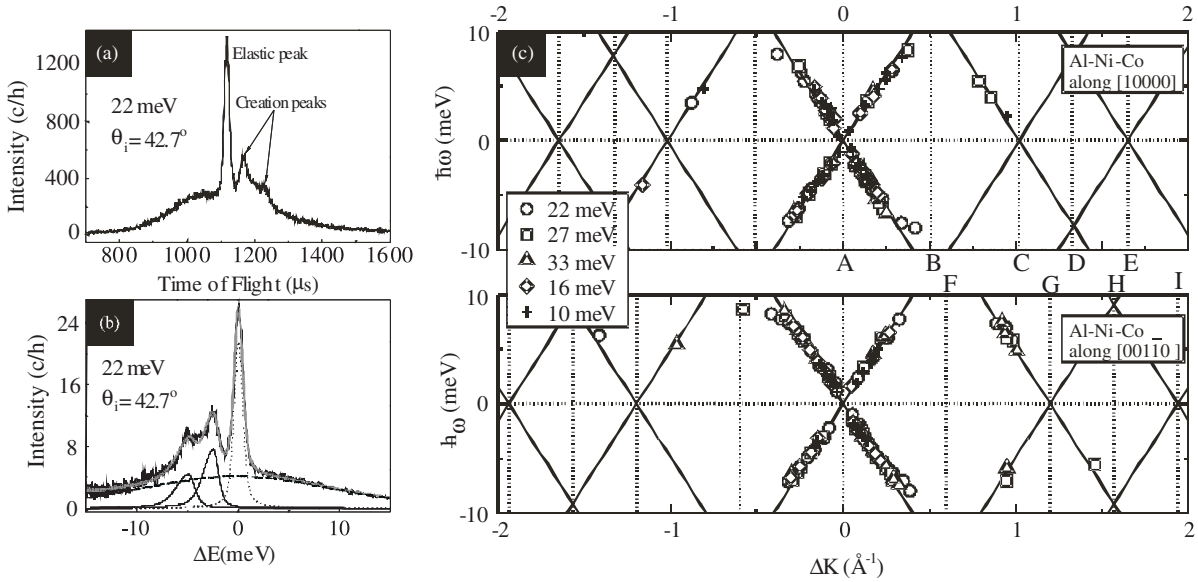

Figure 7. (a) TOF spectrum from the tenfold d-$Al_{71.8}Ni_{14.8}Co_{13.4}$ surface at He atoms incident angle $\theta_i = 42.7°$ in the $[10\bar{1}0]$ azimuth. (b) The spectrum (a) plotted with respect to energy transfer. (For data fitting, different curves were used for elastic peak, background and phonon peaks). (c) Dispersion relation along the high symmetry [10000] and $[10\bar{1}0]$ directions. Different symbols reflect data taken for different beam energies. Solid lines represent the linear dispersion calculated from elastic moduli. Reprinted with permission from [68]. Copyright 2003, American Physical Society.

phonons (Rayleigh mode phonons) on the tenfold surface of d-$Al_{71.8}Ni_{14.8}Co_{13.4}$ and the fivefold surface of i-$Al_{70.5}Pd_{21}Mn_{8.5}$ using inelastic He atom scattering [68]. The Rayleigh waves propagate along the surface with the polarization vector (direction of displacement of atoms) lying in the sagittal plane (the plane defined by the surface normal and propagation direction of the wave).

Phonons in periodic crystals have a well-defined energy and wavevector due to the lattice periodicity and phonon modes can be fully characterized by a wavevector confined to the first Brillouin zone and a band index. Due to the lack of periodicity a Brillouin zone cannot be defined in quasicrystals.

Figure 7(a) shows a TOF spectrum taken from the d-Al–Ni–Co surface for a given angle of incidence and a given beam energy. The spectrum exhibits well-defined single phonon creation peaks (He atom loses energy). Single phonon creation and annihilation peaks collected for a variety of incident angles and He atom energies yield the surface phonon dispersion as shown in figures 7(c) and (d) [68]. The data reveals an acoustic branch (Rayleigh mode) originating from $K = 0$, $K = 1.02$ Å^{-1} (B) for the [10000] direction and at $K = 1.2$ Å^{-1} (D) for the $[00\bar{1}0]$ direction. These points correspond to strong reciprocal lattice points and can be regarded as quasi-Brillouin-zone (QBZ) centres.

The initial slope of the dispersion is in excellent agreement with the Rayleigh velocity, $v_R = 3840$ m s^{-1}, calculated from elastic constants and bulk phonons of d-Al–Ni–Co [69]. The velocity is isotropic for the [10000]- and the $[00\bar{1}0]$-directions. Beyond 0.30 Å^{-1}, a tendency of the dispersion to level off towards the QBZ boundaries can be observed. However, a reliable determination of the phonon energy at the QBZ boundaries is not possible since the single phonon peaks in the TOF spectra vanish in the Gaussian background as they approach the QBZ boundary. Because of these ill-defined phonon peaks for larger wavevectors, it was not possible to determine whether the surface phonon peaks exhibit a strong increase of intrinsic width beyond a specific momentum as observed for bulk phonons.

As with the d-Al–Ni–Co quasicrystal, the i-Al–Pd–Mn quasicrystal exhibits well-defined surface phonons with features expected from the bulk phonons [68].

5. Adsorption and growth

Quasicrystal surfaces have proven an intriguing substrate for adsorption and growth. In contrast to simple periodic surfaces they provide a large range of similar but non-identical local environments for the adsorbing species. Furthermore, they allow us to explore fundamental questions regarding the essence of epitaxial interfaces.

In general for molecular adsorption it is found that at room temperature, either no adsorption takes place [70], or molecules aggressively attack the surface as is the case of oxygen on i-Al–Pd–Mn where an amorphous surface oxide forms [71, 72]. (A recent report indicates that an ordered surface oxide may be formed under appropriate preparation conditions [73].) At low temperatures, benzene (C_6H_6) was found to adsorb in a disordered fashion on i-Al–Pd–Mn [74]. Ethylene (C_2H_4) was used to passivate the tenfold surface of d-Al–Ni–Co in measurements of the friction of the surface using atomic force microscopy [75].

For elemental adsorption, the primary surfaces used have been fivefold i-Al–Pd–Mn and tenfold Al–Ni–Co. It is noteworthy that few adsorption studies predate the year 2000.

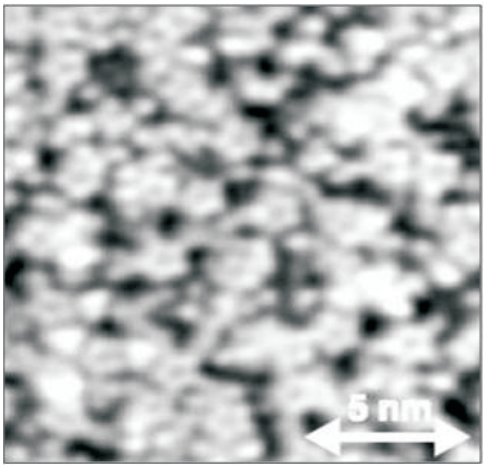

Figure 8. Adsorption of 0.54 ML of Bi on the fivefold surface of i-Al–Pd–Mn at room temperature after [81].

Up to this time most effort had been concentrated in studies of the clean surfaces as discussed in sections 2–7. Of the techniques which have been applied to adsorbate systems STM is predominant. Several surface structural techniques such as surface extended x-ray adsorption fine structure (SEXAFS), and photoelectron diffraction (PhD), although ideally suited to adsorbate site determination in periodic systems, are not readily applicable to adsorption on quasicrystal surfaces due to the multiplicity of possible adsorption sites.

A detailed description of structural results for each system studied is beyond the scope of this paper. The reader is referred to some other recent review articles in this area [8, 9, 30, 38, 76–79]. Below we focus on several topical areas where substantial understanding has been achieved.

5.1. Nucleation and growth of pseudomorphic monolayers

Among the most interesting systems are those where growth occurs pseudomorphically. Several single pseudomorphic monolayers have been identified; these are systems such as fivefold i-Al–Pd–Mn/Bi [80, 81] and fivefold i-Al–Pd–Mn/Pb [82] and tenfold d-Al–Ni–Co/Pb [83].

An example of this is shown in figure 8. This shows the fivefold surface of i-Al–Pd–Mn after adsorption of 0.54 ML of Bi. The Bi atoms nucleate into pentagonal clusters on the surface with about 0.48 nm interatomic separation. This clusters are identified as nucleating at sites corresponding to truncated pseudo-Mackay clusters which have a Mn atom at their centre. The high density of such sites on the surface, which because of their relation to the underlying bulk structure are quasiperiodically ordered, leads to a long-range ordering in the adsorbed layer. When all such sites are occupied with Bi pentagons, the remainder of the available surface is then taken up with Bi atoms and a quasiperiodic monolayer is formed. Annealing the monolayer leads to greater order in the overlayer.

These pentagonal motifs are a feature of several adsorption systems and lead to a pseudomorphic monolayer in the Bi case described above and for Pb adsorption on i-Al–Pd–Mn [82, 84]. Such starfish were also observed for Al on i-Al–Cu–Fe, but did not lead to monolayer growth in that case [85–87].

5.2. Epitaxy between quasiperiodic and periodic structures

Commensurate epitaxial interfaces in periodic materials are characterized by a common interface unit cell. This would not be possible in interfaces with quasiperiodic materials as these do not have a unit cell. Thus, it was held for a long time that epitaxial interfaces between quasiperiodic and periodic materials could not exist. However, it was recently pointed out by Franke *et al* that the requirement of a common interface cell in periodic systems can be viewed as the consequence of a more fundamental characteristic of epitaxial interfaces, namely the 'locking into registry' provided by local minima in the interface energy with regard to relative translations of the respective half-crystals [88]. This was shown to be equivalent to requiring the coincidence of at least two non-collinear interface-projected reciprocal lattice vectors of the two half-crystals. Franke *et al* demonstrated such an epitaxial alignment for AlAs islands formed on a d-Al–Ni–Co high index surface. A detailed discussion of the possible epitaxial matches between periodic materials and different surface orientations of decagonal quasicrystals and the resulting structural properties is given in [89]. One intriguing perspective is the possibility to use quasicrystalline interlayers to epitaxially link materials that are incommensurate.

5.3. Rotational epitaxy

One can adopt a broader view of epitaxy beyond that of thin film and surface science often referring to commensurate interfaces as discussed above. This broader view includes any interfaces with preferential orientations which—when not falling into the commensurate class—are frequently referred to as exhibiting rotational epitaxy.

A typical example of rotational epitaxy is provided in non-commensurate systems with islands of periodic atomic structure oriented along high symmetry directions of a substrate's surface. This mode is adopted by Al and Ag on icosahedral Al–Pd–Mn and decagonal Al–Ni–Co and Fe on icosahedral Al–Pd–Mn [90–92]. Sometimes the adsorbing species will intermix with the quasicrystal substrate, forming an interfacial alloyed rotational epitaxial layer. Only one system tested so far, Gd adsorbed on i-Al–Pd–Mn, has exhibited purely 3D (Volmer–Weber) growth [78].

For those systems that exhibit rotational epitaxial growth, the quasicrystalline/crystalline interface seeks to find the lowest energy configuration. This is achieved by selection of a particular allotrope and crystal orientation of the islands that are formed—for example in the case of Al deposited on the fivefold surface of icosahedral Al–Pd–Mn, the orientation of the islands is such that a [100] axis of the fcc Al lattice coincides with a twofold direction of the icosahedral substrate [93]. A model for the general case of such growth is explained in detail by Widjaja *et al* [94].

An alloyed interfacial layer may also be formed in some cases; this happens in the cases of Ni and Fe on decagonal Al–Ni–Co [95, 96] and Au on decagonal Al–Ni–Co and on icosahedral Al–Pd–Mn [97–99].

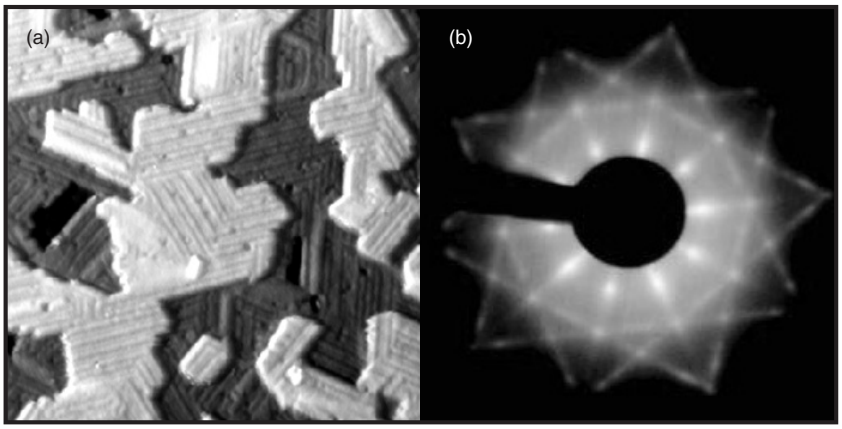

Figure 9. (a) 40 nm × 40 nm STM image of 5.5 ± 0.2 ML Cu adsorbed on the fivefold face of icosahedral Al–Pd–Mn. (b) A LEED pattern taken from this surface at 169 eV. Reprinted with permission from [100]. Copyright 2004, American Physical Society.

5.4. Modulated multilayer structures

Intermediate to the systems in which a quasicrystalline monolayer is observed (with or without the formation of islands at higher coverages) and the systems in which crystalline rotational epitaxial growth is observed there exists a class of growth mode in which the structure of the adsorbate, whilst locally consistent with the usual crystalline form of the element concerned, is modulated on a slightly larger scale with a degree of aperiodic character arising from the quasicrystalline substrate. This growth mode is closer to rotational epitaxial growth than to pseudomorphic growth and may be considered in terms of the coincident reciprocal lattice planes model as an optimization of the film structure in order to achieve a denser coincident site lattice between the quasicrystalline surface and the largely crystalline domains which grow thereon [94]. The modulation, in the two examples that have been observed to date, is on the scale of 1 nm [100–102], and bears a direct correlation to the underlying quasicrystal surface.

Figure 9(a) shows a scanning tunnelling microscopy (STM) image of a Cu film deposited on icosahedral Al–Pd–Mn. The coverage is around 4 ML. Apparent in this STM image is the formation of five orientations of a 'row' structure. The rows themselves are arranged according to the binary Fibonacci sequence with the two separations concerned being of the magnitudes 4.6 and 7.4 Å. These separations are consistent with a Fibonacci pentagrid drawn connecting similar features on the clean quasicrystal surface. There are some phason defects in the film (manifested as non-Fibonacci ordering of the row sequences); it is unclear whether these are also propagated from the underlying quasicrystal surface or are a strain-relieving mechanism of the film. There is also another kind of defect, manifested as lighter rows within the domains, which could be explained in terms of another strain-relieving mechanism. Figure 9(b) shows a low energy electron diffraction (LEED) pattern obtained at low temperature from this film. The streaking of the pattern is due to the high density of Bragg like peaks in reciprocal space from the aperiodic Fibonacci sequence exhibited by the row structure. The periodic separation perpendicular to the streaking direction corresponds to the periodic character of the Cu along the rows [21]. Quantitative structural solutions have been sought using medium energy ion scattering (MEIS) [101] and later LEED(IV) [103]; as yet there is no consensus.

LEED and STM results from a Co film adsorbed on the same substrate and also adsorbed on decagonal Al–Ni–Co indicated that in both cases, for moderate coverages of around 20 ML, the same mode of growth occurred [102]. The film in this case was much less flat and less well-ordered than the lower coverage Cu/Al–Pd–Mn film, and the ordering was of a lower degree of perfection. However, STM results were sufficiently resolved to permit the observation of angular ordering consistent with fivefold symmetry on the moderately-dosed quasicrystal surfaces, and the LEED pattern was broadly similar to that obtained for Cu/Al–Pd–Mn. In this case, the repeat distance along the rows was found to be consistent with hcp Co.

5.5. Rare-gas adsorption

The use of rare gases to study surfaces provides an opportunity to probe the weakly interacting geometric component of the surface potential. As rare gases are chemically inert, the equilibrium positions of adsorbed atoms depend on the corrugation of the surface potential. That said, it has previously been found that Xe can undergo a significant degree of charge transfer to the surface, in certain cases causing a large degree of redistribution of charge within the substrate [104]. This phenomenon can have a strong effect on preferred adsorption sites and in the case of Xe on Cu, results in the atop position [105]. A LEED experiment on the adsorption of Xe on the tenfold surface of quasicrystalline Al–Ni–Co found that the diffraction pattern experienced a reduction in peak intensity up to the completion of monolayer coverage [105]. Thereafter 30 spots per ring were observed at the same value of momentum transfer as the primary substrate peaks. These results are consistent with ten orientations of fcc Xe(111) with high density axes oriented along the ten primary crystal directions of the substrate surface.

Following this work, a theoretical approach was utilized to investigate the structure of the monolayer. It was

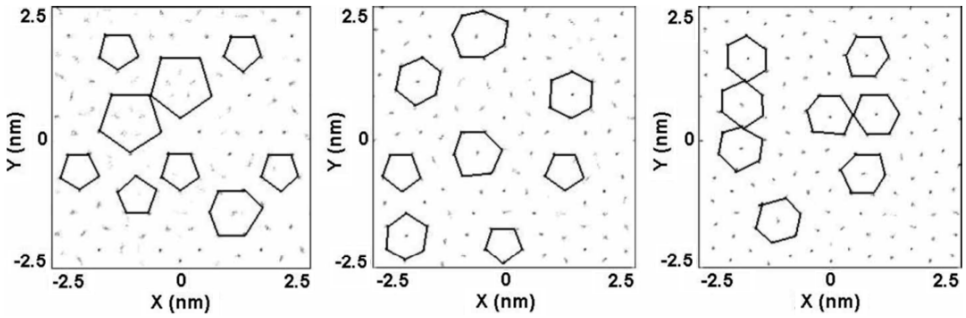

Figure 10. The evolution of the film with increasing density versus lateral size from (a) to (c) as studied with GCMC. Xe atoms are visible as black dots and the substrate is not shown. (a) 3.752 atoms nm^{-2}; many pentagons can be seen, including τ-scaled and inverted pentagons, and there appears to be no other structure visible. The transitional phase is in evidence in (b), 4.938 atoms nm^{-2}, with distorted hexagons and pentagons both visible. Finally, in (c), 5.590 atoms nm^{-2}, the transition to rotational epitaxy is largely complete, with sixfold symmetry dominating though pentagons may still be observed at domain intersections. Reprinted from [106] with permission from Philosophical Magazine.

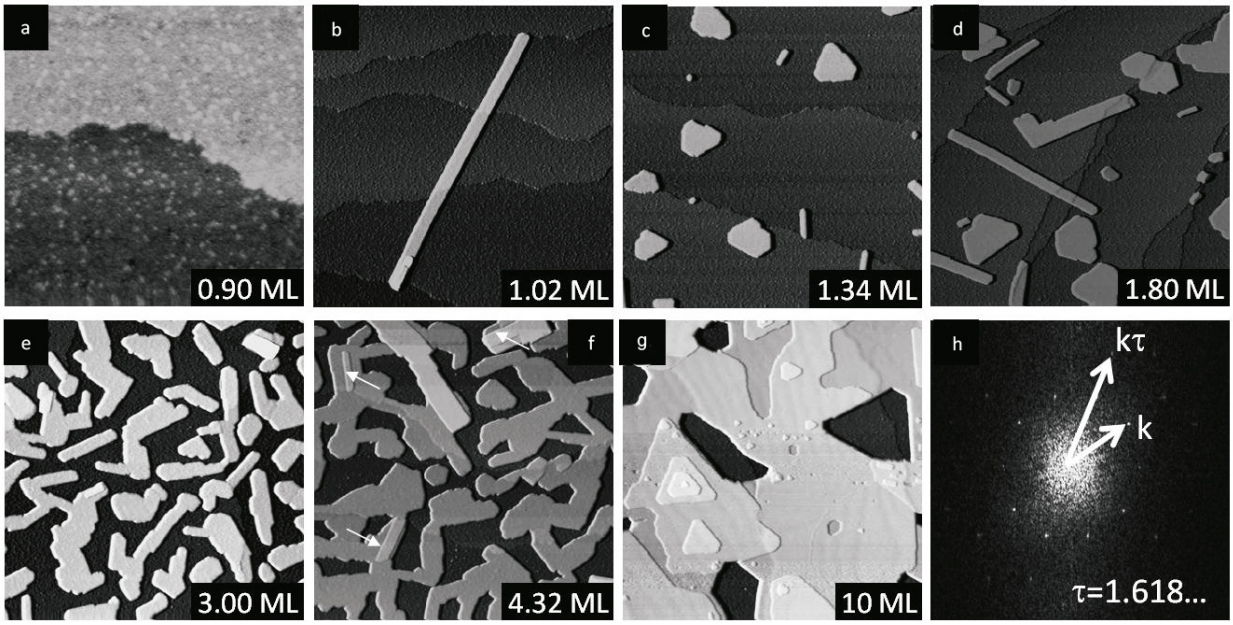

Figure 11. (a)–(g) STM images of the tenfold surface of d-Al–Ni–Co after deposition of Bi at different coverages at room temperature ((a): 80 nm × 80 nm, (b): 300 nm × 300 nm, (c): 400 nm × 400 nm, (d): 300 nm × 300 nm, (e): 250 nm × 250 nm, (f): 250 nm × 250 nm, (g): 200 nm × 200 nm). (h) Fourier transform of image (a). Reprinted with permission from [111]. Copyright 2008, American Physical Society.

found using *ab initio* methods that quasicrystalline Al–Ni–Co exhibits a high degree of corrugation to adsorbing Xe atoms, with the strongest binding energies in the region of 150–250 meV [106], compared to a range for close-packed periodic surfaces between 25 meV (Cs) [107] and 160 meV (graphite) [108]. Subsequent grand canonical Monte Carlo (GCMC) simulations indicated the presence of fivefold symmetry in initial adsorption in the submonolayer regime. As the density increases, the local atomic structure gradually changes from fivefold symmetric to sixfold symmetric. The resulting higher coverage film is close-packed (GCMC results are inconclusive as to whether the structure is fcc or hcp or a combination of both) with a network of pentagonal defects causing domain rotation by 36° in each case [106]. Figure 10 follows growth via the GCMC simulations from low film density to high film density.

5.6. Thin films with magic heights

A number of elements deposited on quasicrystal surfaces develop islands of specific heights, so-called 'magic heights'. The selection of magic heights is interpreted in terms of quantum size effects arising from electron confinement within the film, where the substrate-film and film-vacuum interfaces act as a barrier for the motion of the electrons perpendicular to the surface. Confinement leads to the formation of discrete energy levels—the quantum well states—whose energy is dependent on the film thickness. At thicknesses where these states lie well below the Fermi energy the electronic energy of the film is minimized leading to enhanced stability structural [109, 110].

Sharma *et al* observed magic heights in Bi film deposited on various quasicrystal surfaces. Figure 11 shows STM images from the tenfold d-Al–Ni–Co surface at different

coverages (θ) [8, 111]. For $\theta \leqslant 1$, Bi forms a smooth film with quasicrystalline long-range order (figure 11(a)). The quasicrystalline order is revealed in the Fourier transform which shows tenfold symmetry and maxima located at τ-scaling distances (figure 11(h)). For $1 < \theta < 5$, facetted crystalline islands form with a height of about 1.3 nm, or four layers (4L) of bulk Bi along the [100] direction. Islands of 2L-height and of irregular shape were also observed in the early stages of deposition, but these islands either reshaped themselves into four-atom-high islands or coalesced with neighbouring four-atom-high islands. Above 5 ML, Bi develops triangular islands of monatomic height. The triangular symmetry is expected from the bulk structure of Bi [112]. Both the triangular islands and the 4L-height islands maintain a rotational epitaxial relationship with the substrate.

Bi deposited on the fivefold surface of i-Al–Pd–Mn and i-Al–Cu–Fe surfaces also yield islands of magic heights atop the first quasicrystalline layer. In additional to the predominant 4L-heights, the islands exhibit other heights which are integer multiple of 4L [8].

Fournée *et al* observed by STM that Ag deposited on the fivefold i-Al–Pd–Mn surface at an elevated substrate temperature of 365 K at 1 ML coverage yields islands of different heights. More than 80% of them have 4L- or 5L-height, whereas the remaining 20% of the islands have 1L-, 2L-, 3L-height, suggesting an enhanced stability of 4L- and 5L-high islands. In contrast to the Bi islands formed atop the first wetting layer, Ag islands are formed directly on the bare substrate.

Moras *et al* identified by photoemission spectroscopy the quantum well states in Ag thin films deposited on either the fivefold surface of i-Al–Pd–Mn or the tenfold surface of d-Al–Ni–Co [113], thus confirming the electronic growth mechanism, which was earlier suggested by Fournée *et al* [8]. It was suggested that the confinement may be driven by the incompatible symmetries of the electronic states of the crystalline film and the quasicrystalline substrate.

Sharma *et al* found that Sn deposited on the fivefold surface of i-Al–Cu–Fe at 15 ML coverage yields islands of selected heights [114]. These heights are close to the step heights of the substrate. However, it is not known whether the height selection is related to a quantum size effect.

6. Wider impact

In the preceding sections we have given a snapshot of the state-of-the-art in the field of research on quasicrystal surfaces. However work on quasicrystals has also stimulated interest in what has been a somewhat neglected related area, that of the clean surfaces of giant unit cell complex metallic alloys. In order to compare the behaviour of quasicrystals with that of periodic materials with similar chemical composition, quasicrystal approximants were studied. These are periodic complex metallic alloys with similar composition to quasicrystals, and with a comparable valence electron concentration per atom. They may share structural motifs with the quasicrystals. Most published work has been on the pseudo-tenfold face of the ξ'-Al–Pd–Mn quasicrystal approximant [114–116]. Recently the field has broadened to include other giant unit cell materials not necessarily related to quasicrystals. This includes work on the $Al_{80}Cr_{15}Fe_5$ pseudo-sixfold (100) and pseudodecagonal (010) surfaces [117], the (010) surface of the Taylor phase Al_3(Mn, Pd) [118] and the (010) face of μ-Al_4Mn [119]. Here the STM and LEED data are consistent with the notion that the surfaces are truncations of the bulk structure. The lessons learned from quasicrystal surfaces appear to transfer readily to the study of these giant unit cell materials, and this area appears likely to grow in the coming years.

Quasicrystal surfaces have also provided a unique opportunity for studying aspects of properties such as friction. Friction is a complex phenomenon, with many channels contributing to energy dissipation. Park and co-workers used atomic force microscopy (AFM) and STM to study the twofold surface of d-Al–Ni–Co which contains both periodic and quasiperiodic directions [51, 75, 120]. By measuring the torsional response of the AFM cantilever, they could directly compare frictional effects along the periodic and aperiodic directions on the same surface. A decrease in the torsional response by a factor of eight along the aperiodic direction compared with that along the periodic direction indicates that periodicity may be a significant factor in determining friction of materials. The authors suggest that the lower friction along the aperiodic direction may be due to a low possibility of energy dissipation through phonon generation.

The study of quasicrystal surfaces and overlayers has led to several developments in how experimental and theoretical techniques are applied at surfaces. For example for the analysis of LEED I(V) data, Gierer, van Hove *et al* implemented several approximations in the LEED analysis code in order to model the experimental data successfully [19, 121]. More recently, experimental data from d-Al–Ni–Co has been modelled using calculations from approximant models [122]. In this case, no modifications are needed to the LEED code although the large size of the unit cell means the calculations are computationally intensive. The necessity for consistent interpretation of STM results has also led to new areas of application of DFT. The approach is similar to that described in the paragraph above for the LEED techniques. As described in section 2.1 DFT calculations have been performed on surface slabs of approximants derived from models of the bulk structure. STM simulations from the resulting structure agree extremely well with actual STM images of the surface [33]. A final area where the study of quasicrystal surfaces has had impact is on image analysis in STM. The lack of periodicity in the surface structure has led to the extensive implementation of image analysis techniques such as Fourier filtering and autocorrelation. Some of these applications are described elsewhere [4]; it is likely that such techniques could find wider applicability in the broad surface science community.

7. Concluding remarks

For clean surfaces of quasicrystals, techniques have been developed which allow the preparation of flat surfaces with a step-terrace morphology. In all studies, evidence has emerged

that the surfaces prepared in this fashion are structurally similar to what would be expected from bulk truncations, that is there is no evidence of structural reconstruction taking place (though identifying a reconstruction from diffraction data or through Fourier transform of STM images if the reconstruction were τ-scaled would not be impossible). The combination of STM and DFT looks promising in understanding details of the surface structure. The challenge of understanding the surface structure of these materials has also given rise to technique developments, particularly for quantitative studies using LEED I(V). Nonetheless there is still a paucity of quantitative structural determinations, and the restriction to Al-based materials is unfortunate. The study of the Ag-based quasicrystals [54], while in its infancy, is a promising new direction. The number of reports of studies of the clean surfaces of giant unit cell materials looks set to increase. More studies using quantitative techniques such as surface x-ray diffraction (SXRD) would be welcome.

In adsorption and epitaxy on quasicrystals, several new phenomena such as multilayer modulation [100], pseudomorphic monolayers [80] and quantum size effects [8] have been observed. Such studies have furthered our understanding of epitaxy in general. The discovery of pseudomorphic monolayer systems provides us with single element quasiperiodic surfaces whose properties can be compared directly with periodic clean surfaces or surfaces of thin films of the same element. While surface investigations have up until very recently focussed on quasicrystals where Al has been the main component, the investigation of the new Ag–In–Yb P-type icosahedral quasicrystals will extend the literature in this respect. Looking forward, there are significant unmapped regions of the adsorbate landscape which will undoubtedly lead to interesting new phenomena in growth.

Acknowledgments

We acknowledge the European Network of Excellence on Complex Metallic Alloys (CMA) contract NMP3-CT-2005-500145 and EPSRC (grant numbers EP/D05253X/1 and EP/D071828/1) for financial support. Steve Barrett of the University of Liverpool is acknowledged for his development of the ImageSXM image analysis software suite /www.liv.ac.uk/∼sdb/ImageSXM/ used in many of the studies described above.

References

[1] Shechtman D, Blech I, Gratias D and Cahn J W 1984 *Phys. Rev. Lett.* **53** 1951
[2] Binning G, Rohrer H, Gerber Ch and Weibel E 1982 *Phys. Rev. Lett.* **49** 57
[3] Kortan A R, Becker R S, Thiel F A and Chen H S 1990 *Phys. Rev. Lett.* **64** 200
[4] McGrath R, Leung L, Barrett S D and Ledieu J 2005 *Proc. R. Microsc. Soc.* **40** 215
[5] McRae E G, Malic R A, Lalonde T H, Thiel F A, Chen H S and Kortan A R 1990 *Phys. Rev. Lett.* **65** 883
[6] Schaub T M, Bürgler D E, Güntherodt H J and Suck J B 1994 *Phys. Rev. Lett.* **73** 1255
[7] Papadopolos Z, Kasner G, Ledieu J, Cox E J, Richardson N V, Chen Q, Diehl R D, Lograsso T A, Ross A R and McGrath R 2002 *Phys. Rev.* B **66** 184207
[8] Fournée V, Sharma H R, Shimoda M, Tsai A P, Unal B, Ross A R, Lograsso T A and Thiel P A 2005 *Phys. Rev. Lett.* **95** 155504
[9] Sharma H R, Shimoda M and Tsai A P 2007 *Adv. Phys.* **56** 403
[10] Bolliger B, Erbudak M, Vvedensky D D, Zurkirch M and Kortan A R 1998 *Phys. Rev. Lett.* **80** 5369
[11] Shen Z, Kramer M J, Jenks C J, Goldman A I, Lograsso T, Delaney D, Heinzig M, Raberg W and Thiel P A 1998 *Phys. Rev.* B **58** 9961
[12] Bolliger B, Erbudak M, Hensch A and Vvedensky D D 2000 *Mater. Sci. Eng.* A **294–296** 859
[13] Naumović D, Aebi P, Schlapbach L and Beeli C 2000 *Mater. Sci. Eng.* A **294–296** 882
[14] Bolliger B, Erbudak M, Hensch A, Kortan A R and Vvedensky D D 1999 *Mater. Res. Soc. Symp. Proc.* **553** 257
[15] Ledieu J, Munz A W, Parker T M, McGrath R, Diehl R D, Delaney D W and Lograsso T A 1999 *Surf. Sci.* **435** 666
[16] Ebert Ph, Feuerbacher M, Tamura N, Wollgarten M and Urban K 1996 *Phys. Rev. Lett.* **77** 3827
[17] Ledieu J, Dhanak V R, Diehl R D, Lograsso T A, Delaney D W and McGrath R 2002 *Surf. Sci.* **512** 77
[18] Ledieu J, Muryn C A, Thornton G, Cappello G, Chevrier J, Diehl R D, Lograsso T A, Delaney D W and McGrath R 2000 *Mater. Sci. Eng.* A **294** 871
[19] Gierer M, Van hove M A, Goldman A I, Shen Z, Chang S L, Pinhero P J, Jenks C J, Anderegg J W, Zhang C M and Thiel P A 1998 *Phys. Rev.* B **57** 7628
[20] Jenks C J, Ross A R, Lograsso T A, Whaley J A and Bastasz R 2002 *Surf. Sci.* **521** 34
[21] Ledieu J, Hoeft J T, Reid D E, Smerdon J A, Diehl R D, Ferralis N, Lograsso T A, Ross A R and McGrath R 2005 *Phys. Rev.* B **72** 035420
[22] Barbier L, Le Floc'h D, Calvayrac Y and Gratias D 2002 *Phys. Rev. Lett.* **88** 085506
[23] Sharma H R, Fournée V, Shimoda M, Ross A R, Lograsso T A, Tsai A P and Yamamoto A 2004 *Phys. Rev. Lett.* **93** 165502
[24] Ledieu J, Cox E J, McGrath R, Richardson N V, Chen Q, Fournée V, Lograsso T A, Ross A R, Caspersen K J, Unal B, Evans J W and Thiel P A 2005 *Surf. Sci.* **583** 4
[25] Shen Z, Stoldt C R, Jenks C J, Lograsso T A and Thiel P A 1999 *Phys. Rev.* B **60** 14688
[26] Ledieu J, McGrath R, Diehl R D, Lograsso T A, Delaney D W, Papadopolos Z and Kasner G 2001 *Surf. Sci.* **492** L729
[27] Unal B, Lograsso T A, Ross A R, Jenks C J and Thiel P A 2005 *Phys. Rev.* B **71** 165411
[28] Unal B, Jenks C J and Thiel R A 2008 *Phys. Rev.* B **77** 195419
[29] Gratias D, Puyraimond F, Quiquandon M and Katz A 2000 *Phys. Rev.* B **63** 024202
[30] Ledieu J and McGrath R 2003 *J. Phys.: Condens. Matter* **15** S3113
[31] Krajčí M and Hafner J 2005 *Phys. Rev.* B **71** 184207
[32] Unal B, Jenks C J and Thiel P A 2009 *J. Phys.: Condens. Matter* **21** 055009
[33] Krajčí M, Hafner J, Ledieu J and McGrath R 2006 *Phys. Rev.* B **73** 024202
[34] Tsai A P 2003 *Acc. Chem. Res.* **36** 31
[35] Sharma H R, Franke K J, Theis W, Riemann A, Fölsch S, Gille P and Rieder K H 2004 *Phys. Rev.* B **65** 235409
[36] Gierer M, Mikkelsen A, Gräber M, Gille P and Moritz W 2000 *Surf. Sci. Lett.* **463** L654
[37] Kishida M, Kamimura Y, Tamura R, Edagawa K, Takeuchi S, Sato T, Yokoyama Y, Guo J Q and Tsai A P 2002 *Phys. Rev.* B **65** 094208

[38] McGrath R, Ledieu J, Cox E J and Diehl R D 2002 *J. Phys.: Condens. Matter* **14** R119
[39] Yuhara J, Klikovits J, Schmid M, Varga P, Yokoyama Y, Shishido T and Soda K 2004 *Phys. Rev.* B **70** 024203
[40] Ferralis N, Pussi K, Cox E J, Gierer M, Ledieu J, Fisher I R, Jenks C J, Lindroos M, McGrath R and Diehl R D 2004 *Phys. Rev.* B **69** 153404
[41] Steurer W and Haibach T 1999 *The Physics of Quasicrystals* ed Z M Stadnik (Heidelberg: Springer)
[42] Steurer W, Haibach T, Zhang B, Kek S and Lück R 1993 *Acta Crystallogr.* B **49** 661
[43] Yamamoto A and Weber S 1997 *Phys. Rev. Lett.* **78** 4430
[44] Hiragara K, Ohsuna T, Sun W and Sugiyama K 2001 *Mater. Trans., JIM* **42** 2354
[45] Tröger H 1999 *PhD Thesis*
[46] Suzuki T, Sharma H R, Nishimura T, Shimoda M, Yamauchi Y and Tsai A-P 2005 *Phys. Rev.* B **72** 115427
[47] Sharma H R, Franke K J, Theis W, Riemann A, Fösch S, Gille P and Rieder K H 2004 *Surf. Sci.* **561** 121
[48] Becker R S, Kortan A R, Thiel F A and Chen H S 1991 *J. Vac. Sci. Technol.* B **9** 867
[49] Krajčí M, Hafner J and Mihalkovič M 2006 *Phys. Rev.* B **73** 134203
[50] Sharma H R, Theis W, Gille P and Rieder K H 2002 *Surf. Sci.* **511** 387
[51] Park J Y, Ogletree D F, Salmeron M, Ribeiro R A, Canfield P C, Jenks C J and Thiel P A 2005 *Science* **309** 1354
[52] Park J Y, Ogletree D F, Salmeron M, Ribeiro R A, Canfield P C, Jenks C J and Thiel P A 2005 *Phys. Rev.* B **72** 220201
[53] Maeder R, Widmer R, Groening P, Deloudi S, Steurer W, Heggen M, Schall P, Feuerbacher M and Groening O 2009 *Phys. Rev.* B at press
[54] Sharma H R, Shimoda M, Ohhashi S and Tsai A P 2007 *Phil. Mag.* **87** 2989
[55] Sharma H R, Shimoda M, Sagisaka K, Takakura H, Smerdon J A, Nugent P J, McGrath R, Ohhashi S and Tsai A P 2008 submitted
[56] Sharma H R, Shimoda M and Tsai A P 2006 *Japan. J. Appl. Phys.* **45** 2208
[57] Mori M, Matsuo S, Ishimasa T, Matsuura T, Kamiya K, Inokuchi H and Matsukawa T 1991 *J. Phys.: Condens. Matter* **3** 767
[58] Stadnik Z M, Zhang G W, Tsai A-P and Inoue A 1995 *Phys. Rev.* B **51** 4023
[59] Wu X, Kycia S W, Olson C G, Benning P J, Goldman A I and Lynch D W 1995 *Phys. Rev. Lett.* **75** 4540
[60] Stadnik Z M, Purdie D, Garnier M, Baer Y, Tsai A P, Inoue A, Edagawa K and Takeuchi S 1996 *Phys. Rev. Lett.* **77** 1777
[61] Neuhold G, Barman S R, Horn K, Theis W, Ebert P and Urban K 1998 *Phys. Rev.* B **58** 734
[62] Fujiwara T, Mitsui T and Yamamoto S 1996 *Phys. Rev.* B **53** R2910
[63] Smith A P and Ashcroft N W 1987 *Phys. Rev. Lett.* **59** 1365
[64] Theis W, Rotenberg E, Franke K J, Gille P and Horn K 2003 *Phys. Rev.* B **68** 104205
[65] Rotenberg E, Theis W, Horn K and Gille P 2000 *Nature* **406** 602
[66] Burkov S E, Timusk T and Ashcroft N W 1992 *J. Phys.: Condens. Matter* **4** 9447
[67] Rotenberg E, Theis W and Horn K 2002 *J. Alloys Compounds* **342** 348
[68] Sharma H R, Franke K J, Theis W, Gille P, Ebert Ph and Rieder K H 2003 *Phys. Rev.* B **68** 054205
[69] Swenson C A, Fisher I R, Anderson J N E and Canfield P C 2002 *Phys. Rev.* B **65** 184206
[70] McGrath R, Ledieu J, Cox E J, Haq S, Diehl R D, Jenks C J, Fisher I, Ross A R and Lograsso T A 2002 *J. Alloys Compounds* **342** 432
[71] Chang S L, Chin W B, Zhang C M, Jenks C J and Thiel P A 1995 *Surf. Sci.* **337** 135
[72] Chang S L, Anderegg J W and Thiel P A 1996 *J. Non-Cryst. Solids* **195** 95
[73] Longchamp J N, Erbudak M and Weisskopf Y 2007 *Appl. Surf. Sci.* **253** 5947
[74] Hoeft J T, Ledieu J, Haq S, Lograsso T A, Ross A R and McGrath R 2006 *Phil. Mag.* **86** 869
[75] Park J Y, Ogletree D F, Salmeron M, Ribeiro R A, Canfield P C, Jenks C J and Thiel P A 2005 *Phys. Rev.* B **71** 144203
[76] Diehl R D, Ledieu J, Ferralis N, Szmodis A W and McGrath R 2003 *J. Phys.: Condens. Matter* **15** R63
[77] Thiel P A 2008 *Annu. Rev. Phys. Chem.* **59** 129
[78] Smerdon J A, Wearing L H, Parle J K, Leung L, Sharma H R, Ledieu J and McGrath R 2008 *Phil. Mag.* **88** 2073
[79] Smerdon J A, Sharma H R, Ledieu J and McGrath R 2008 *J. Phys.: Condens. Matter* **20** 314005
[80] Franke K J, Sharma H R, Theis W, Gille P, Ebert P and Rieder K H 2002 *Phys. Rev. Lett.* **89** 156104
[81] Smerdon J A, Parle J K, Wearing L H, Lograsso T A, Ross A R and McGrath R 2008 *Phys. Rev.* B **78** 075407
[82] Ledieu J, Leung L, Wearing L H, McGrath R, Lograsso T A, Wu D and Fournée V 2008 *Phys. Rev.* B **77** 073409
[83] Smerdon J A, Leung L, Parle J K, Jenks C J, McGrath R, Fournée V and Ledieu J 2008 *Surf. Sci.* **602** 2496
[84] Ledieu J, Krajci M, Hafner J, Leung L, Wearing L H, McGrath R, Lograsso T A, Wu D and Fourne V 2009 *Phys. Rev.* B **79** 165430
[85] Cai T, Ledieu J, McGrath R, Fournée V, Lograsso T A, Ross A R and Thiel P A 2003 *Surf. Sci.* **526** 115
[86] Ghosh C, Liu D J, Schnitzenbaumer K J, Jenks C J, Thiel P A and Evans J W 2006 *Surf. Sci.* **600** 2220
[87] Ghosh C, Liu D J, Jenks C J, Thiel P A and Evans J W 2006 *Phil. Mag.* **86** 831
[88] Franke K J, Gille P, Rieder K-H and Theis W 2007 *Phys. Rev. Lett.* **99** 036103
[89] Theis W and Franke K J 2008 *J. Phys.: Condens. Matter* **20** 314004
[90] Bolliger B, Dmitrienko V E, Erbudak M, Lüscher R, Nissen H U and Kortan A R 2001 *Phys. Rev.* B **6305** 052203
[91] Flückiger T, Weisskopf Y, Erbudak M, Lüscher R and Kortan A R 2003 *Nano Lett.* **3** 1717
[92] Fournée V, Ross A R, Lograsso T A, Evans J W and Thiel P A 2003 *Surf. Sci.* **537** 5
[93] Lüscher R, Erbudak M and Weisskopf Y 2004 *Surf. Sci. Rep.* **569** 163
[94] Widjaja E J and Marks L D 2008 *J. Phys.: Condens. Matter* **20** 314003
[95] Weisskopf Y, Erbudak M, Longchamp J N and Michlmayr T 2006 *Surf. Sci.* **600** 2592
[96] Wearing L H, Smerdon J A, Leung L, Dhesi S S, Ledieu J, Bencok P, Fisher I, Jenks C J and McGrath R 2008 *J. Phys.: Condens. Matter* **20** 015005
[97] Shimoda M, Sato T J, Tsai A P and Guo J Q 2000 *Phys. Rev.* B **62** 11288
[98] Shimoda M, Guo J Q, Sato T J and Tsai A P 2001 *Japan. J. Appl. Phys.* **40** 6073
[99] Noakes T C Q, Bailey P, Draxler M, McConville C F, Ross A R, Lograsso T A, Leung L, Smerdon J A and McGrath R 2006 *J. Phys.: Condens. Matter* **18** 5017
[100] Ledieu J, Hoeft J T, Reid D E, Smerdon J A, Diehl R D, Lograsso T A, Ross A R and McGrath R 2004 *Phys. Rev. Lett.* **92** 135507
[101] Smerdon J A, Ledieu J, McGrath R, Noakes T C Q, Bailey P, Drexler M, Mcconville C F, Lograsso T A and Ross A R 2006 *Phys. Rev.* B **74** 035429
[102] Smerdon J A, Ledieu J, Hoeft J T, Reid D E, Wearing L H, Diehl R D, Lograsso T A, Ross A R and McGrath R 2006 *Phil. Mag.* **86** 841
[103] Pussi K, Reid D E, Ferralis N, McGrath R, Lograsso T A, Ross A R and Diehl R D 2008 *Phil. Mag.* **88** 2103

[104] Silva L F Da, Stampfl C and Sheffler M 2003 *Phys. Rev. Lett.* **90** 066104
[105] Caragiu M, Seyller T and Diehl R D 2003 *Surf. Sci. Rep.* **539** 165
[106] Diehl R D, Ferralis N, Pussi K, Cole M W, Setyawan W and Curtarolo S 2006 *Phil. Mag.* **86** 863
[107] Chizmeshya A, Cole M W and Zaremba E 1998 *J. Low Temp. Phys.* **110** 677
[108] Vidali G, Ihm G, Kim H-Y and Cole M W 1991 *Surf. Sci. Rep.* **12** 133
[109] Chiang T-C 2000 *Surf. Sci. Rep.* **39** 181
[110] Milun M, Pervan P and Woodruff D P 2002 *Rep. Prog. Phys.* **65** 99
[111] Sharma H R, Fournee V, Shimoda M, Ross A R, Lograsso T A, Gille P and Tsai A P 2008 *Phys. Rev.* B **78** 10
[112] Nagao T, Sadowski J T, Saito M, Yaginuma S, Fujikawa Y, Kogure T, Ohno T, Hasegawa Y, Hasegawa S and Sakurai T 2004 *Phys. Rev. Lett.* **93** 105501
[113] Moras P, Weisskopf Y, Longchamp J-N, Erbudak M, Zhou P H, Ferrari L and Carbone C 2006 *Phys. Rev.* B **74** 121405(R)
[114] Sharma H R, Shimoda M, Fournée V, Ross A R, Lograsso T A and Tsai A P 2005 *Phys. Rev.* B **71** 224201
[115] Fournée V, Ross A R, Lograsso T A, Anderegg J W, Dong C, Kramer M, Fisher I R, Canfield P C and Thiel P A 2002 *Phys. Rev.* B **66** 165423
[116] Cecco C, Barth C, Gille P, Feuerbacher M, Krausch G and Reichling M 2004 *J. Non-Cryst. Solids* **334** 491
[117] Smerdon J A, Parle J K, McGrath R, Bauer B and Gille P 2009 *Z. Kristallogr.* **224** 13
[118] Addou R, Deniozou T, Gaudry E, Heggen M, Feuerbacher M, Widmer R, Gröning O, Fournée V, Dubois J M and Ledieu J 2009 in preparation
[119] Widmer R, Maeder R, Heggen M, Feuerbacher M and Gröning O 2008 *Phil. Mag.* **88** 2095
[120] Park J Y, Ogletree D F, Salmeron M, Ribeiro R A, Canfield P C, Jenks C J and Thiel P A 2006 *Phys. Rev.* B **74** 024203
[121] Gierer M, Van hove M A, Goldman A I, Shen Z, Chang S L, Jenks C J, Zhang C M and Thiel P A 1997 *Phys. Rev. Lett.* **78** 467
[122] Pussi K, Ferralis N, Mihalkovič M, Widom M, Curtarolo S, Gierer M, Jenks C J, Canfield P, Fisher I R and Diehl R D 2006 *Phys. Rev.* B **73** 184203